THE MICROSTRUCTURE OF HIGH STRENGTH BLAST FURNACE SLAG CONCRETE

Tarja Häkkinen
LicTech, Senior Research Scientist
Technical Research Centre of Finland
Building Materials Laboratory
P.O.Box 26 (Kemistintie 3)
SF-02150 ESPOO

ABSTRACT

The microstructures of the blended cement concrete, alkali activated slag concrete and Portland cement concrete were compared. The structures of the samples and the compositions of the hardening products were investigated by means of porosity studies, optical and scanning electron microscopy, thermoanalysis and X-ray studies.

In the alkali activated and auto activated slag concrete the structure contains microcracks at the microscopic level. According to the SEM studies the hardened structure of alkali activated glassy slag is composed of smooth granular products, while the fibre type hardening products are lacking.

Key words: blast furnace slag, high strength, microcracks, microstructure.

1 INTRODUCTION

The influence of the binder type on the permeability and microstructural properties of high strength concrete was studied. High strength Portland cement concrete, blended cement concrete and alkali activated slag concrete were compared with each other. The results of the permeability studies are presented in the first part of the study (Häkkinen 1992). The effect of the content and type of activator on the microcracks was studied. The reasons for the cracking tendency in alkali activated slag concrete were discussed on the basis of SEM studies.

2 MATERIALS

The chemical compositions of the cementitious materials are presented in Table 1. The surface area of the granulated blast furnace slag (GS) was 770 m^2/kg (Blaine).

Table 1 The oxide composition of the cementitious materials

	OXIDE COMPOSITION (% by weight) Ground granulated slag (GS)	Rapid hardening Portland cement (PC)
CaO	39.1	60.1
SiO_2	35.1	20.4
Al_2O_3	8.8	4.9
MgO	10.1	3.5
Fe_2O_3	2.0	2.6
SO_3	0.36	3.4
Insoluble	0.80	0.87
Ignition loss(950°C)	2.2	0.0

3 DRYING SHRINKAGE

The influence of the binder type on the drying shrinkage was studied. Rapid hardening Portland cement, blended cement and alkali activated slag were compared with each other. The shrinkage measurements were performed on mortar specimens measuring 40 x 40 x 160 mm. The water binder ratio was 0.35 and the aggregate binder ratio was 3. The maximum size of aggregate was 2 mm. The specimens were cured in water (T=40°C) for 3 weeks. After that the specimens were dried in desiccators above a saturated sodium nitrite solution. The ambient air in desiccators was mixed by fans. After 2 months' drying one of the desiccators was flushed with CO_2 - air mixture ($CO_2 \approx 5\%$) once a day. The shrinkage of the specimens was followed by demec measurements for 6 months (Table 2). The shrinkage process continued longer in alkali activated slag specimens than in Portland cement specimens. The compressive strengths of the specimens were also determined (Table 3).

The carbonation depths of the specimens were determined by thin section analysis, after the specimens had been cured for 6 months in the desiccator (2 months sheltered + 4 months CO_2). The carbonation depths of the Portland cement and the blended cement (GS+PC) samples were about 2 mm and in the alkali activated slag concrete (AA GS) samples about 5 mm. Microcracks appeared not in the PC samples, a few in the GS+PC samples and a number in the AA GS samples. The proceeding of carbonation along the microcracks was observed in the AA GS samples. It was

concluded that the microcracks were not generated in the course of thin section preparation.

Table 2 Shrinkage of the mortar specimens. Mean of 16 values (4 surfaces of 4 specimens).

Binder	Curing	SHRINKAGE (%) Drying period (months) 2	4	6
PC *	sheltered	0.043	0.041	0.043
GS+PC **	sheltered	0.031	0.034	0.041
AA GS ***	sheltered	0.033	0.052	0.069
PC	CO_2	-	0.043	0.049
GS+PC	CO_2	-	0.034	0.040
AA GS	CO_2	-	0.054	0.065

* Rapid hardening Portland cement.
** 70% (by w. of binder) blast furnace slag 30 % rapid hardening Portland cement
*** Blast furnace slag activated by NaOH (3% by w. of binder).

Table 3 Compressive strength of the mortar specimens. Mean for 6 values.

Curing	COMPRESSIVE STRENGTH (MPa±SD) PC	GS+PC	AA GS
2 months sheltered	80.9 (3.7)	71.4 (8.5)	75.2 (1.2)
12 months sheltered	131.0 (6.1)	122.8 (8.8)	106.7 (1.9)
2 months sheltered, 10 months CO_2	136.0 (12.9)	130.7 (5.1)	135.8 (7.9)

4 PORE SIZE DISTRIBUTION

The effects of carbonation on the pore size distribution were studied with paste specimens. The water binder ratio was 0.3. The binding materials were as follows:
- rapid hardening Portland cement (PC)
- GS (70% by w. of binder) and PC (30% by w. of binder)
- GS activated by NaOH (3% by w. of slag).

The specimens were cured in water (T=40°C) for 3 weeks in order to achieve a high hydration degree. Thereafter the specimens

were cured in desiccators as described in paragraph 3. After 6 months' curing in desiccators the surface samples were vacuum dried. Pore size distribution curves for the samples were determined using mercury porosimetry at the Laboratory for Fuel and Process Technology of the Technical Research Centre of Finland. In the calculations the contact angle between the material and mercury was assumed to be 141.3°. The appearance of the pores in 3 pore size areas was studied. The results are presented in Table 4.

Table 4 Porosity of the paste samples.

Binder and curing	POROSITY (10^{-3} x cm^3/g) AND SHARE OF TOTAL POROSITY (%) Pore radius (nm) 10,000 - 100	100 - 50	50 - 10	TOTAL POROSITY (10^{-3} x cm^3/g)
PC sheltered	1.3 4%	22.3 60%	13.5 36%	37
PC CO_2	5.0 18%	4.3 16%	18.3 66%	28
GS+PC sheltered	10.5 33%	2.8 9%	18.5 58%	32
GS+PC CO_2	4.5 23%	1.0 5%	13.8 71%	19
AA GS sheltered	12.8 35%	4.3 12%	19.4 53%	36
AA GS CO_2	13.5 44%	5.3 17%	11.7 38%	30

The influence of carbonation on the pore size distribution was also studied with surface samples from the mortar specimens. The cementitious materials of the mortars were the same as in the paste specimens. The water-binder ratio of the mortar was 0.56 and the aggregate-binder ratio 3. Quartz sand with the maximum particle size of 2 mm was used as the aggregate. The mortar samples were moist cured for 3 months sheltered from carbonation and thereafter for 6 months either in a desiccator above a saturated salt solution (RH≈70%) sheltered from carbonation or in the carbonation chamber (CO_2≈3%, RH≈70%). The carbonation depth was measured by dyeing with using phenolphtalein solution (Table 5). According to the results the samples sheltered from carbonation were not carbonated. The carbonation depth and the appearance of microcracking was also studied by means of fluorescence and polarising microscopy (Table 6).

Table 5 Carbonation depth of the specimens measured by dyeing.
6 months'curing in accelerated carbonation conditions.

Binder	CARBONATION DEPTH (mm) Accelerated carbonation
PC	4
GS+PC	6
AA GS	20

Table 6 Summary of the microscopy examination.
6 months'curing in accelerated carbonation conditions.

Binder	CARBONATION DEPTH (mm)	MICROCRACKING 0-3 0 = no microcracks
PC	6	0
GS+PC	6	0.5
AA GS	20	2

The pore size distribution of the samples was determined with mercury porosimetry at the Technical University of Helsinki. In each case two parallel samples were examined. Samples of 10 mm in height were taken from the surface of the mortar specimens. The samples were vacuum dried for 6 weeks.

The PC samples sheltered from carbonation showed mainly 30-80 nm pores. The number of 5-30 nm pores in the carbonated samples was a little higher and the number of 30-1000 nm pores was a little lower than in the sheltered samples (Figs. 1 and 2).

The GS+PC samples sheltered from carbonation showed a predominance of 5-50 nm pores. In carbonated samples the number of 20-100 nm pores was a little fewer than in sheltered samples. Correspondingly the total porosities of the carbonated samples were less than the total porosities of sheltered samples (Figs. 3 and 4).

The AA GA samples sheltered from carbonation showed a predominance of 5-10 nm pores and 2000-3000 nm pores. In the carbonated samples the volume of 5-10 nm pores had decreased and the volume of 10-1000 nm pores had increased compared to the sheltered samples (Figs 5 and 6).

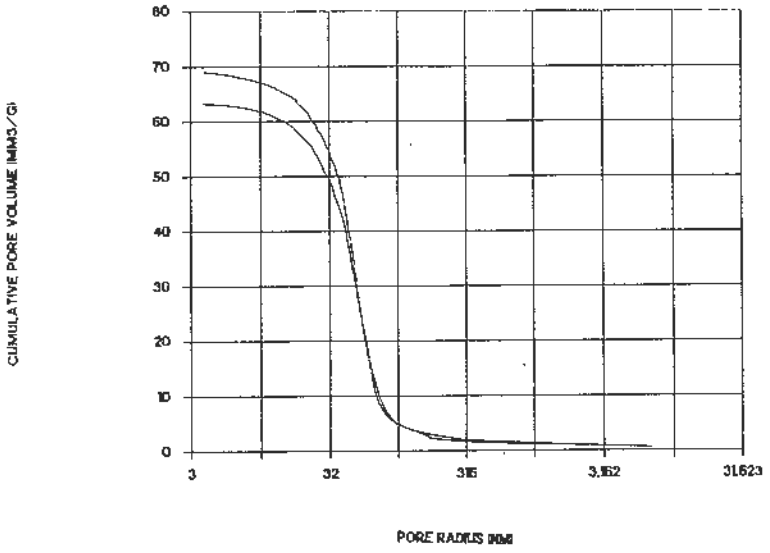

Fig. 1 Pore size distribution of PC mortar.Curing in desiccator.

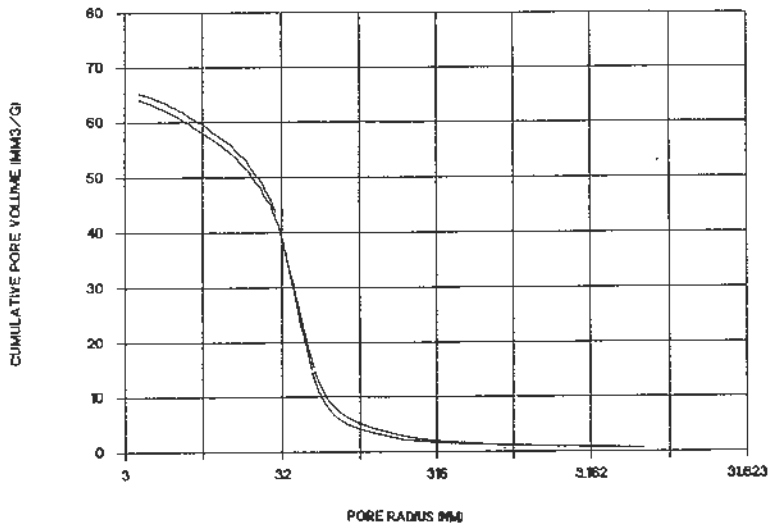

Fig. 2 Pore size distribution of PC mortar.Curing in CO_2 chamber.

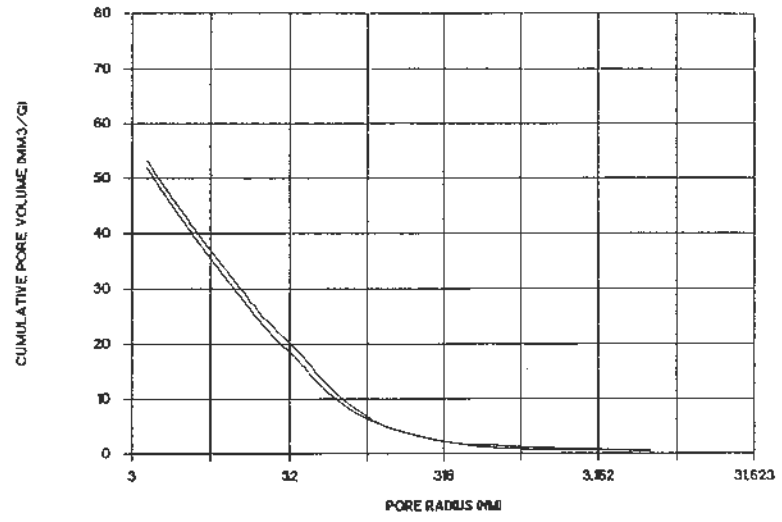

Fig. 3 Pore size distribution of PC+GS mortar. Curing in desiccator.

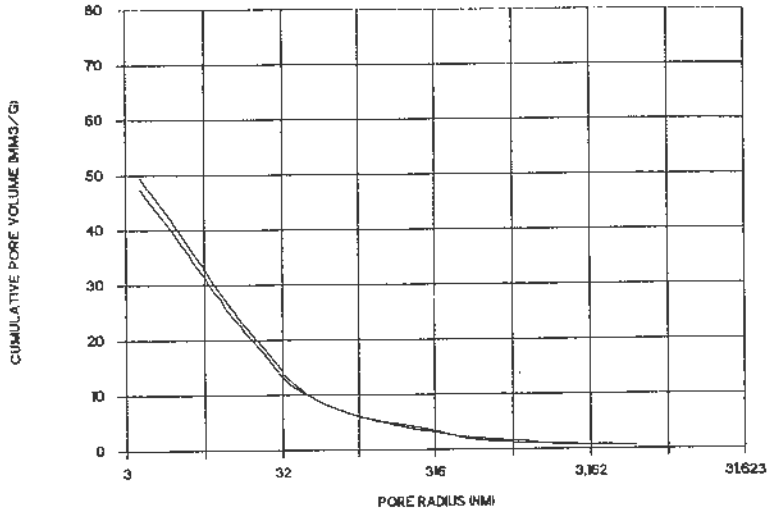

Fig. 4 Pore size distribution of PC+GS mortar.Curing IN CO_2 chamber.

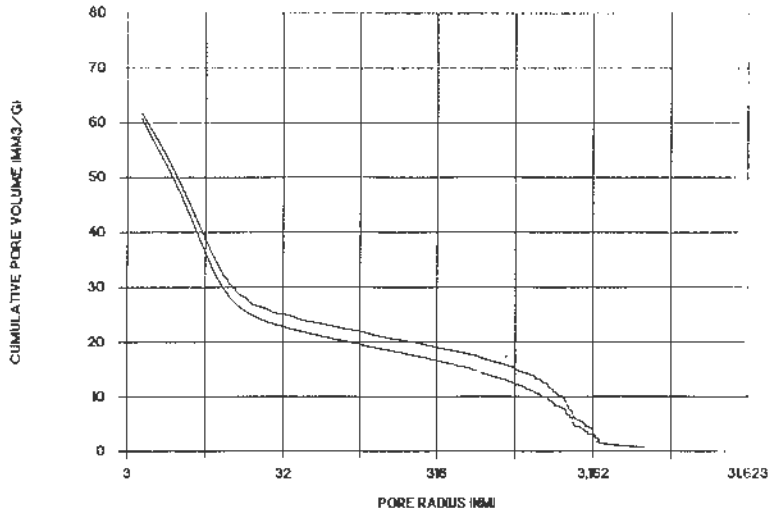

Fig. 5 Pore size distribution of GS+ NaOH mortar. Curing in desiccator.

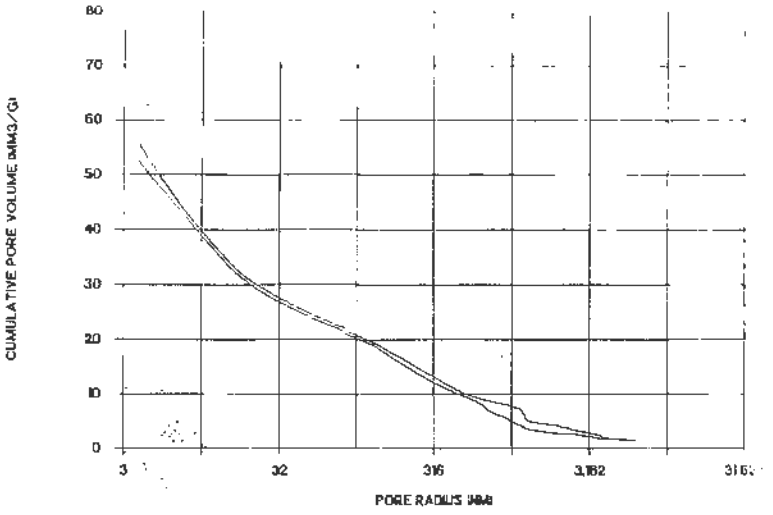

Fig. 6 Pore size distribution of GS+ NaOH mortar.Curing in CO_2 chamber.

The surface samples were also studied thermoanalytically. The samples were taken from the surface and from 2 mm's, 10 mm's and 20 mm's depth in a specimen. 2A Netzsch STA 429 thermobalance was used. The pulverized powders were heated in the thermobalance up to 1050°C using a heating rate of 10°C/min. The heating took place in nitrogen atmosphere with Al_2O_3 powder as a reference material. Both the sample and the reference material were in Al_2O_3 crucibles. In the samples the disintegration occurred in the temperature range 450-850°C. The area was exceptionally large. Possibly, all the carbonates did not appear as calcium carbonates, but also hydrocarbonates were created. The content of carbonates in the surface samples was calculated, assuming that they were all bound as calcium carbonates (Table 7). It was observed that the carbonation degree was lower in PC mortar than in GS70 and in AA GS mortar and that in the surface layers the mole ratio CO_2(chem.bound)/CaO(binder) was 0.8 both in the alkali activated slag mortar and in the Portland cement mortar.

Table 7 The content of carbonates as calcium carbonates.

Binder	Content of carbonates (by w. of sample) The distance from the surface of the specimen		
	Surface	10 mm	20 mm
PC	20.4	2.2	2.3
GS70	15.8	3.2	1.7
AA GS	13.8	12.9	12.8

5 SPECIFIC SURFACE AREA AND APPEARANCE OF THE HARDENING PRODUCTS

The effect of the binder type on the appearance of the hardening products was investigated by means of scanning electron microscopy (Jeol 820). The specific surface areas were determined by nitrogen absorption (Micromeritics Flowsorb 2300). The cementitious materials were as follows:

- rapid hardening Portland cement
- ground granulated blast furnace (70% by w.) and PC (30% by w.)
- alkali activated (NaOH 3% by w. of binder) blast furnace slag.

Paste specimens measuring 40 x 40 x 160 mm were prepared. The water binder ratios were 0.3. 0.4, 0.5 and 0.6. The specimens were cured in water. During the curing cracks appeared onto the surfaces of the AA GS paste specimens. The intensity of the cracking increased as the water binder ratio decreased.

The specific surface areas of the paste samples are presented in Table 8. Before the determination the samples were vacuum dried.

Table 8 Specific surface areas of the paste samples.

Age	SPECIFIC SURFACE AREA (m^2/g) Binder	Water binder ratio 0.4	0.5	0.6
1 day	PC		12.4	12.6
	GS+PC		12.4	-
	AA GS		7.5	10.3
6 days	PC		16.4	25.9
	GS+PC		12.4	19.2
	AA GS	6.2	9.2	14.8
15 days	PC		16.3	22.2
	GS+PC		14.6	18.1
	AA GS		9.6	13.8

The appearance of the hydration products was investigated at early stages of hydration (6 hours and 24 hours) and later at the ages of 4 months and 9 months (Figs. 7 - 13). During the first day a plenty of fibrous and needle like material appeared in the PC paste . In addition calcium hydroxide crystals were observed. On the other hand, the appearance of the AA GS paste was smooth and grain-like. The fibrous material was lacking. At late ages the structures of both the PC and AA GS pastes were densified, but the significant differences with regard to the fibrous material were still to be seen. In the AA GS pastes the edges of the cracks were sharp, but in the PC paste the fibrous material always protruded into the cracks. Typically, a plenty of crystalline $Ca(OH)_2$ appeared around the air pores, but in the AA GS pastes the walls of the air pores were even. The differences between the PC paste and the GS+PC paste were remarkably small compared to those between the PC paste and the AA GS paste. In the GS+PC paste there appeared a plenty of fibrous material although the structure was some what more granular than that of the PC paste.

The paste samples were also studied thermoanalytically. The test arrangements are presented in paragraph 4. The thermoanalytical results revealed that PC activated slag binds calcium in the course of hydration. X-ray diffraction studies were performed using a Philips APD 1700 diffractometer and Cu K_α radiation the voltage being 50 kV and the current 20 mA. The interpretation of the results concerning the AA slag paste is difficult, because the content of crystalline material is remarkably lower than in the PC paste. The highest peaks were caused by a compound, which was some hydration product of slag, possibly $C_5S_6H_5$.

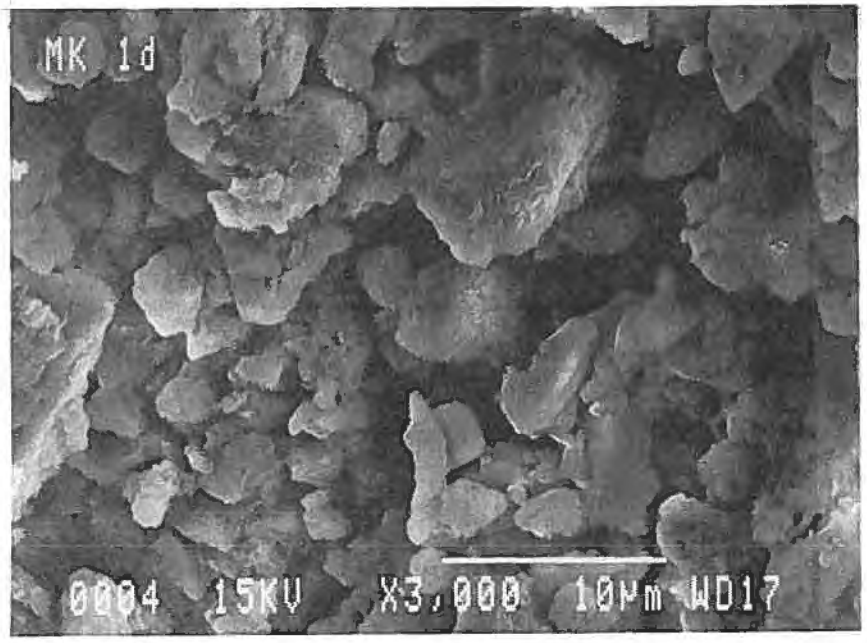

Fig. 7 Alkali activated GS paste. Water binder ratio 0.4. Age 1 day. Magnification x3000.

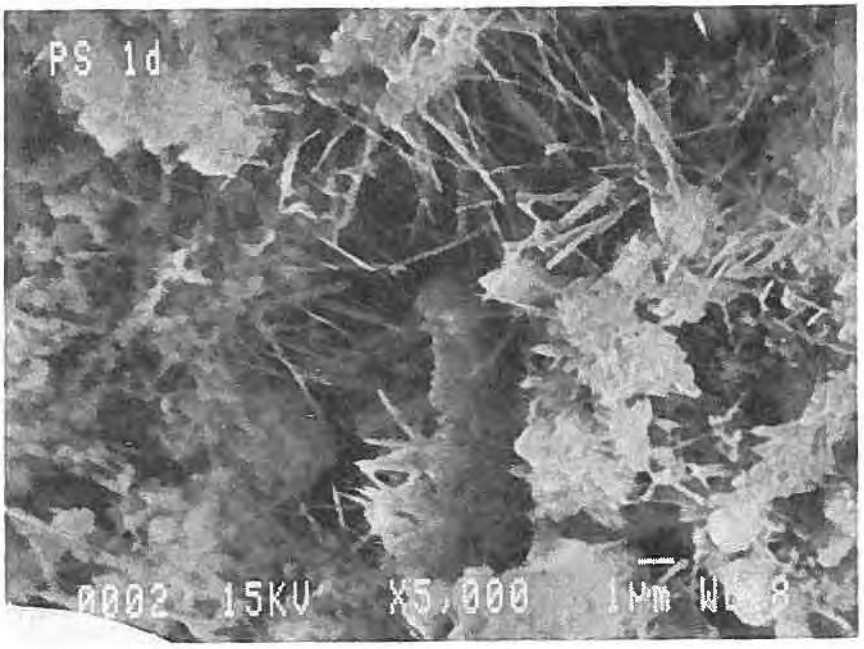

Fig. 8 Portland cement paste. Water binder ratio 0.4. Age 1 day. Magnification x5000.

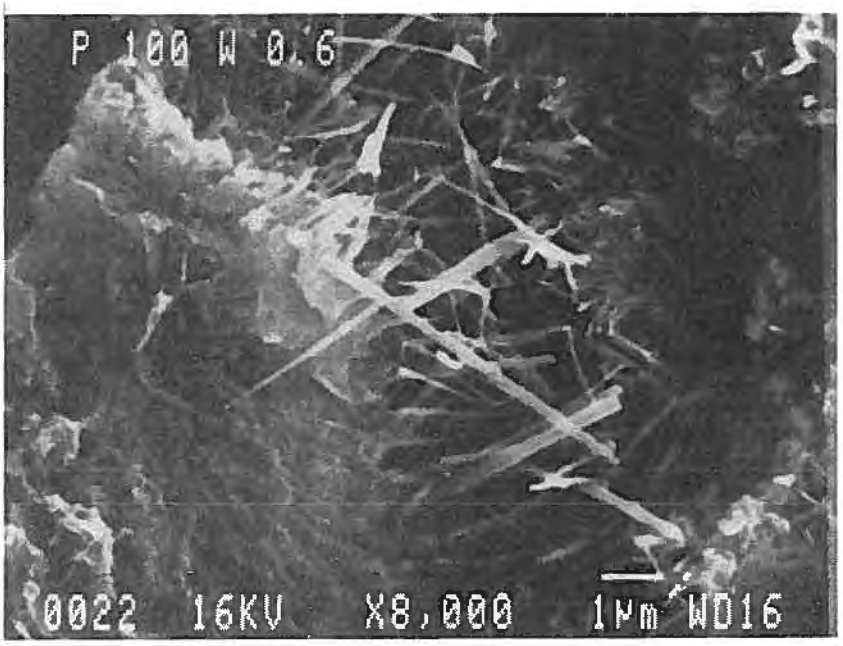

Fig. 9 Portland cementpaste. Water binder ratio 0.6. Age 9 months. Magnification x8000.

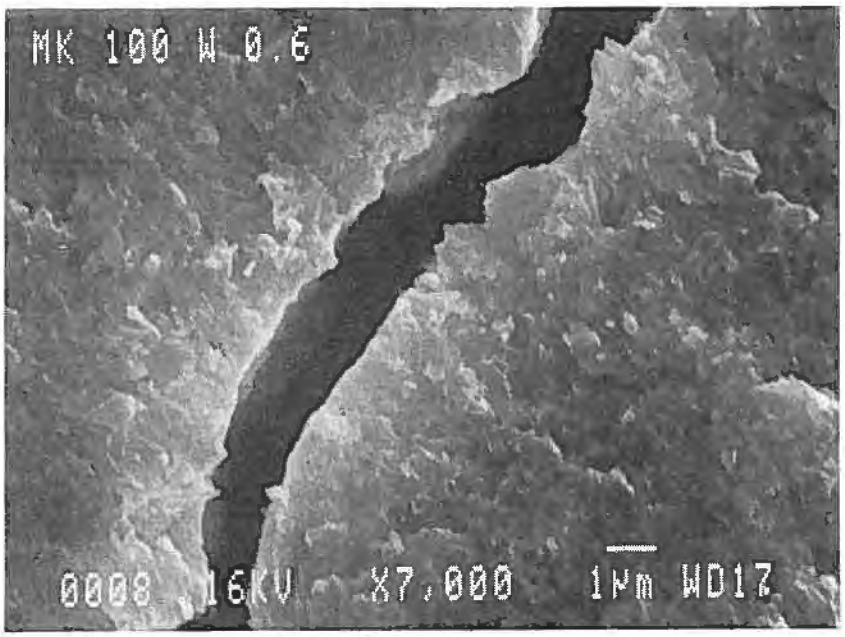

Fig. 10 Alkali activated GS paste. Water binder ratio 0.6. Age 9 months. Magnification x7000.

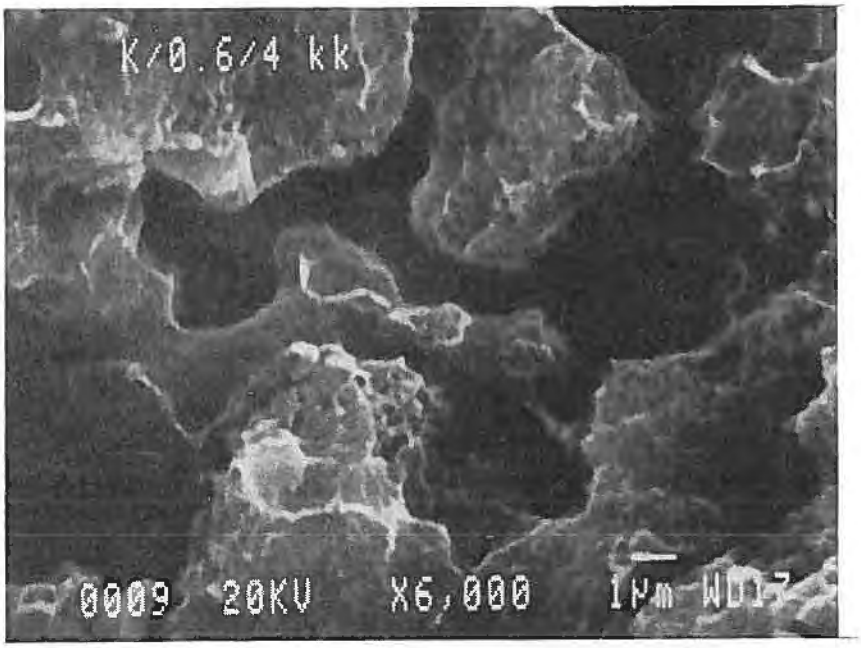

Fig. 11 Alkali activated GS paste. Water binder ratio 0.6. Age 4 months. Magnification x6000.

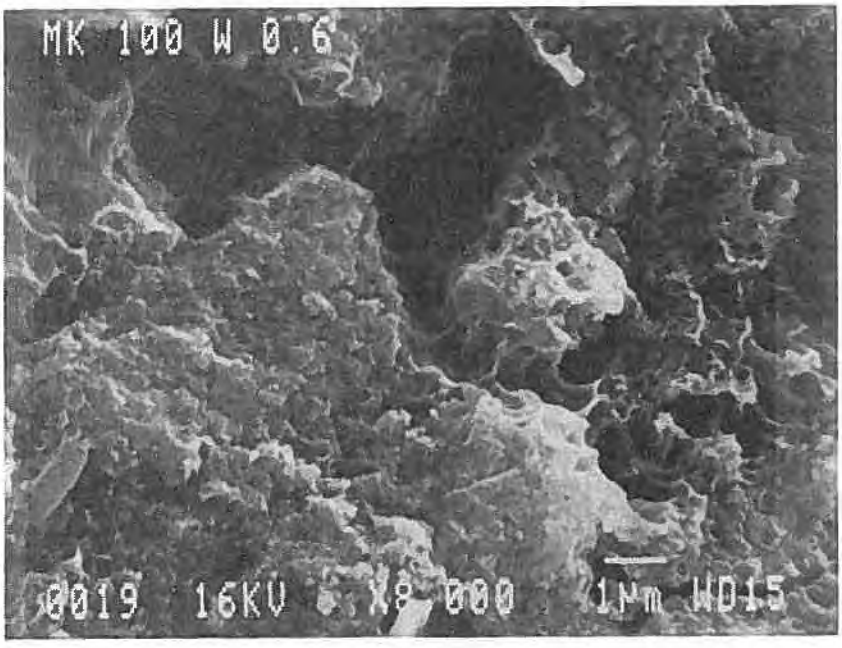

Fig. 12 Alkali activated GS paste. Water binder ratio 0.6. Age 9 months. Magnification x8000.

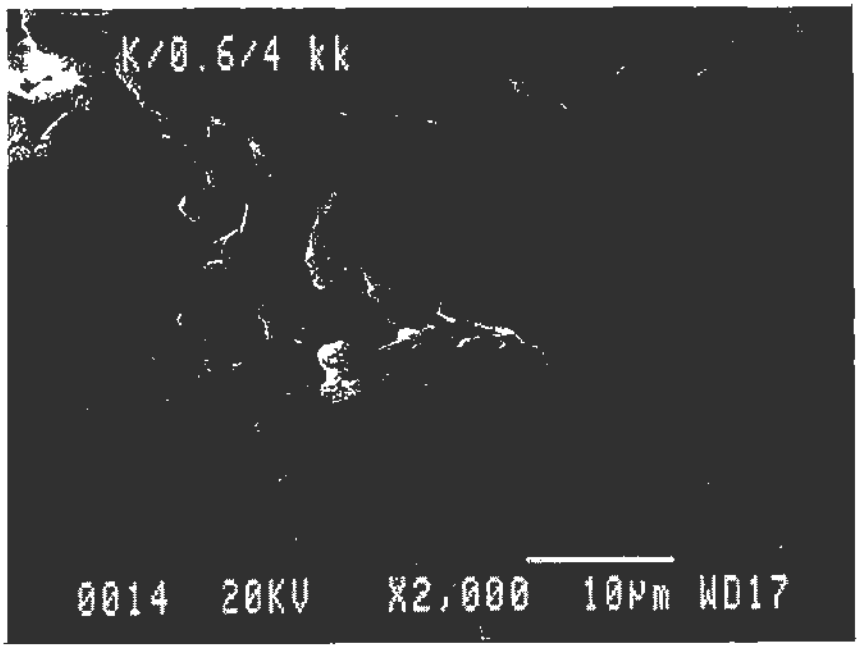

Fig. 13 Alkali activated GS paste. Water binder ratio 0.6. Age 4 months. Magnification x2000. Surface of an air pore.

6 EFFECT OF THE ALKALINE ACTIVATOR ON THE MICROCRACKING

The effect of the type and amount of alkali activator was investigated by means of thin section analysis. The water binder ratio was either 0.30 or 0.38 and the aggregate binder ratio was 3. The maximum aggregate size was 10 mm. Concrete specimens measuring 40 x 40 x 160 mm were heat cured for 6 h at 60°C and moist cured (RH>95%, T=20°C) for 7 days. Thin sections measuring 30 x 50 mm x 25µm impregnated by fluorescent resin were prepared and studied by fluorescent microscopy. The activators under consideration were as follows:

- NaOH and KOH
- amounts of alkali compounds:
  0, 0.8, 2.3 and 3.9 Na_2O equ.% by weight of slag (GS).

The microscopy studies revealed that microcracks appeared in the both KOH and NaOH activated samples. The microcracks were greater in number and size in samples with a high activator content than in those with a low activator content. Microcracks appeared also in the slag concrete sample, which had hardened without activators. There were a few more microcracks in the NaOH activated sample made with a water binder ratio 0.30 than in the corresponding sample made with a water binder ratio 0.38. The compressive strengths were also determined. The results are presented in Table 9.

Table 9 Compressive strength of the concrete specimens. Mean of 6 values.

Activator	Content	Water binder ratio	COMPRESSIVE STRENGTH (MPa+-SD)
NaOH	0	0.38	11.7 (0.78)
NaOH	1	0.38	16.1 (0.48)
NaOH	3	0.38	28.1 (0.54)
NaOH	5	0.38	33.4 (8.0)
NaOH	3	0.30 *	55.6 (0.79)
KOH	1.4	0.38	13.5 (0.54)
KOH	7	0.38	38.6 (0.71)

* Water reducing agent Scancem SP 62 2% by w. of binder.

DISCUSSION AND SUMMARY

The calcium silicate minerals of PC produce crystalline $Ca(OH)_2$ and weakly crystallized calcium-silicate hydrate (CSH). The characteristic morphological types of the gel produced in the PC hydration are classified by Diamond (1976). According to Diamond (1986) a membrane is formed on the surface of the cement particles in the early stage of hydration. The membrane consists mainly of CSH. It can also contain $Ca(OH)_2$, mono sulphonate plates and ettringite needles, which are directed outwards or inwards. The hydration continues as CSH consisting of longitudinal particles (Type 1) and long ettringite needles are precipitated on the surfaces of the membranes reducing the space between the grains (Glasser 1989). Other materials such as CSH Type 2 (reticular network) precipitate in the spaces and an intergrain skeletal structure starts to develop (Diamond 1986). The continual skeleton consisting of the hydration products binds the membranes to form a three dimensional network.

The microstructure of hardened blast furnace slag was studied. According to the results of the SEM studies the hardened structure of alkali activated glassy slag is composed of smooth granular and reticular or honeycomb products, while the fibre-type hardening products are lacking. In the AA GS pastes the edges of the cracks were sharp, but in the PC paste the fibrous material always protruded into the cracks. Typically a plenty of crystalline $Ca(OH)_2$ appeared around the air pores in the PC pastes, but in the AA GS pastes the walls of the air pores were even. The differences between the PC paste and the GS+PC paste where small. In the GS+PC paste a plenty of fibrous material appeared although the structure was somewhat more granular than that of the PC paste.

The microscopy studies revealed that microcracks appeared in both the KOH and NaOH activated and in the auto activated slag samples. The microcracks were greater in number and size in

samples with a high activator content than in those with a low activator content. Microcracks appeared also in the slag concrete sample, which had hardened without activators. The number of cracks was lower in the PC and in the GS+PC concretes than in the AA GS concrete. On the basis of the thin section analysis of carbonated samples it could be concluded that the cracks in AA GS samples are not generated in the course of preparation. Typically, the carbonation had proceeded along the cracks and penetrated also deeper into the sample than the main carbonation zone.

It was concluded that the cracking tendency in the AA GS concrete may be due to the low deformation abilities of the granular material lacking fibrous material. In the early stages of hydration, when the strength of matrix is low, microcracks can be formed due to the hardening deformations. The formation and the growth of cracks is prevented later, when the strength of the matrix increases. In spite of the microcracks, high strength AA GS concrete could be proportioned. In static loading the effects of microcracks can be minor, if the cracks are small and if the strength of the matrix is high. The larger the crack, the higher is the stress peak at the crack, and the weaker is the matrix, the easier the crack growth proceeds.

The reasons for the granular type of matrix and the lack of fibrous material were beyond the scope. The reasons could be the low calcium content in the hardening products or the low crystal content. The AA GS produces low calcium gel. In the microstructural studies a low calcium hydration product of the slag, possibly $C_5S_6H_5$, was observed. The thermoanalytical results revealed that PC-activated GS binds calcium in the course of hydration.

The average pore sizes increased in the AA GS samples cured for 6 months in accelerated carbonation conditions compared to the samples sheltered from carbonation. The pore sizes did not increase in PC or in GS70 samples. However, the carbonation degree of the Portland cement and blended cement concretes remained lower than that was in AA GS samples. Drying shrinkage of the AA GS concrete was significantly greater than that of the PC concrete. The difference was smaller in sheltered conditions than in accelerated carbonation conditions, possibly because of the growth of pore sizes in the AA GS paste due to carbonation. The specific surface areas were smaller in the AA GS pastes than in the PC pastes. This in consistent with the results achieved in the SEM studies.

REFERENCES

Diamond, S. 1976. Cement paste microstructure - an overview at several levels. In: Hydraulic cement pastes: their structure and properties. Proceedings of a Conference held in Sheffield 1976. pp. 2-23.

Diamond, S. 1986. Cement paste microstructure in concrete. In: Microstructural Development During Hydration of Cement.

Materials Research Society Symposia Proceedings. Boston 1986. Vol. 85. pp. 21-32.

Glasser, F.P. et al. 1987. Hydration reactions in cement pastes incorporating fly ash and other pozzolanic materials.In: Microstructural Development During Hydration of Cement. Materials Research Society Symposia Proceedings. Boston 1986. Vol. 85. pp. 167-186.

Häkkinen, T. 1992. The permeability of high strength blast furnace slag concrete. Nordic Concrete Research. Publication No. 10.